ELSEVIER

Global and Planetary Change 15 (1997) 61–77

GLOBAL AND PLANETARY CHANGE

Global warming and active-layer thickness: results from transient general circulation models

Oleg A. Anisimov [a], Nikolai I. Shiklomanov [b], Frederick E. Nelson [b,*]

[a] *Department of Climatology, State Hydrological Institute, 2nd Line V.O., 23, 199053 St. Petersburg, Russia*
[b] *Department of Geography, University of Delaware, Newark DE 19716, USA*

Received 18 December 1996; accepted 23 June 1997

Abstract

The near-surface thermal regime in permafrost regions could change significantly in response to anthropogenic climate warming. Because there is only a small lag between these two processes, the impact of warming on the active layer can be investigated using relatively simple climate-driven models. A formulation attributable to Kudryavtsev was used to study the potential increase of active-layer thickness in the permafrost regions of the Northern Hemisphere, where warming is predicted to be more pronounced than elsewhere. Kudryavtsev's solution was validated using contemporary data, and successfully reproduced the actual depths of frost and thaw at widely spaced locations in North America and Eurasia. Modern climatic data and scenarios of climate change for 2050, derived from three transient coupled ocean–atmosphere general circulation models (GCMs), were used in conjunction with the thaw-depth solution to generate hemispheric maps showing contemporary active-layer thickness for several soil types and moisture conditions, and its relative changes over the next century. The simulations indicate a 20–30% increase of active-layer thickness for most of the permafrost area in the Northern Hemisphere, with the largest relative increases concentrated in the northernmost locations. © 1997 Elsevier Science B.V.

Keywords: active layer; Arctic region; climate change; frost action; global warming; permafrost

1. Introduction

Climatic change is one of the more important problems facing human activities in the high latitudes. Most climate-change scenarios suggest that warming will be amplified and will occur rapidly in the polar regions (Budyko and Izrael, 1987; Maxwell and Barrie, 1989; Roots, 1989; MacCracken et al., 1990), particularly in the permafrost regions, which currently occupy nearly one fourth of the earth's land area.

Permafrost, defined as any subsurface earth materials remaining below 0°C for more than two years, may be affected profoundly by global warming. Most maps use a classification in which permafrost is represented on the basis of its lateral continuity (e.g., Heginbottom et al., 1993; Anisimov et al., 1995). Increases in air

* Corresponding author. Tel.: +1 (302) 831-2294; fax: +1 (302) 832-6654; e-mail: fnelson@udel.edu

PII S0921-8181(97)00009-X

temperature and precipitation may cause thinning or disappearance of permafrost in the *sporadic permafrost zone*, where current climatic conditions produce near-zero annual surface temperatures. Farther poleward, in the *extensive* and *continuous* zones, where permafrost is generally thicker and colder, it may experience substantial warming and become more discontinuous. Such changes in permafrost distribution could have important impacts on northern ecology, forestry, agriculture, hydrology, and engineered works. To address these problems at the hemispheric scale, attempts have been made to model the distribution of permafrost under conditions of changing climate (Nelson and Anisimov, 1993; Anisimov and Nelson, 1996, 1997).

For most practical applications in engineering and ecology, the immediate reaction of near-surface layers of permafrost and seasonally frozen ground are of primary importance (Chapin et al., 1992; Andersland and Ladanyi, 1994; Williams, 1995; Reynolds and Tenhunen, 1996). The thickness of the *active layer*, a layer of soil or other earth materials between the atmosphere and permafrost subject to freezing and thawing on an annual basis, is an extremely important factor in polar ecology. Because most exchanges of energy, moisture, and gases between the atmospheric and terrestrial systems occur through it, thickening of the active layer could have an important effect on geomorphic, hydrologic, and biological processes (Nelson et al., 1993; Weller et al., 1995). At locations where the uppermost permafrost is rich in ground ice, thickening of the active layer could have severe destabilizing effects on engineered works (Fig. 1) and could trigger the release of significant amounts of greenhouse gases to the atmosphere (Fukuda, 1994; Michaelson et al., 1996).

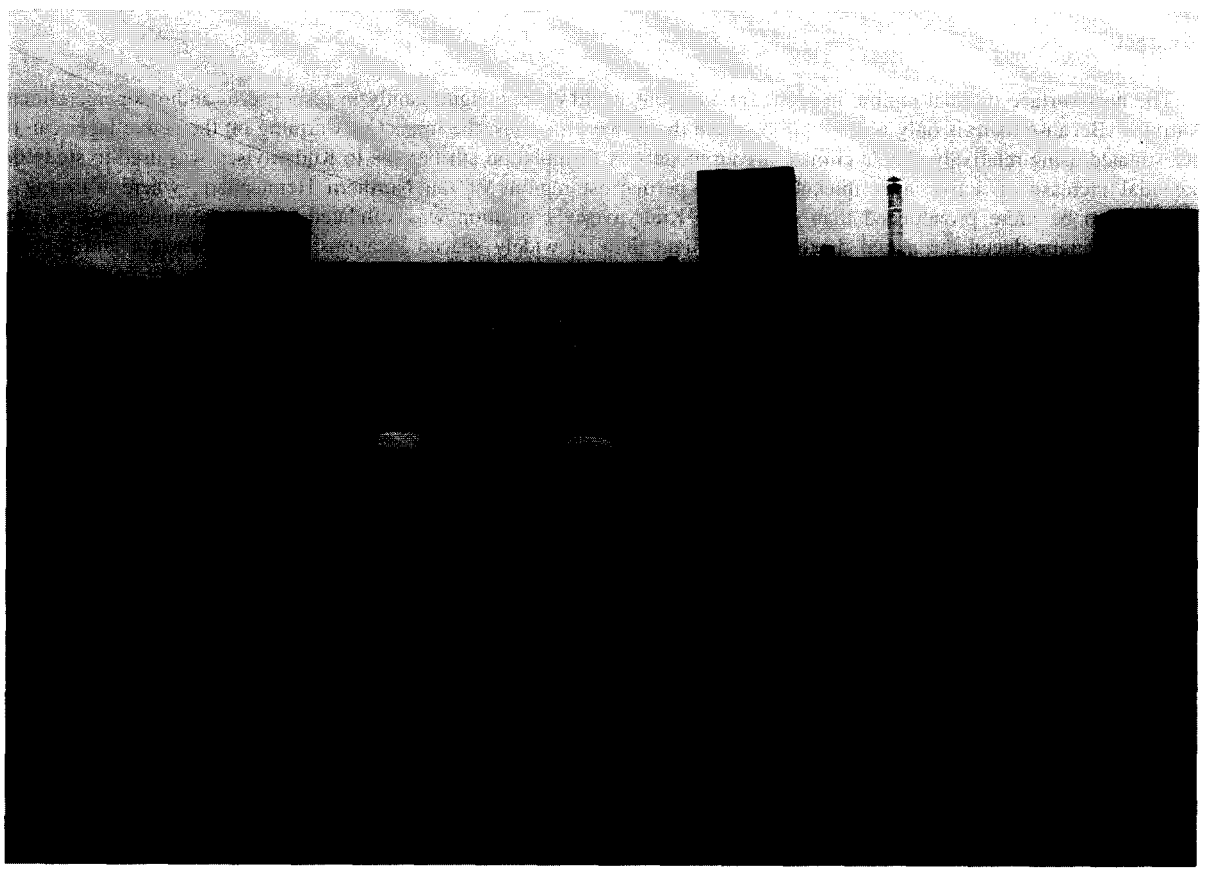

Fig. 1. Building in Faro (Yukon Territory, Canada) undergoing differential settlement due to inappropriate construction practice and consequent thawing of ice-rich upper layers of permafrost. Climatic warming in the high latitudes could result in similar, widespread damage to the infrastructure.

The objectives of this paper are: (1) to utilize a climate-driven analytic model to make generalized predictions of active-layer thickness, at the hemispheric scale; (2) to compare modeled results with contemporary data from locations within the permafrost areas; and (3) to run the model in conjunction with climate-change scenarios and to develop predictive hemispheric maps showing relative changes of active-layer depth by the middle of the next century.

2. Permafrost and seasonal thawing

Empirical field studies have traditionally dominated many aspects of geocryological studies. Much of this work is confined to specific locations where measurements are performed; only a few recent attempts have been made to standardize permafrost data and to compile a highly detailed geocryological map at the hemispheric scale (Heginbottom et al., 1993). Computationally derived maps of permafrost distribution based on theoretical considerations are even fewer at this scale. The 'frost index' (Nelson and Outcalt, 1987) provides one such approach; this dimensionless number is based on the ratio of the annual degree-day sums above and below 0°C, modified to account for the conductive effects of snowcover and other optional parameters. Significant improvements in the availability of climatic and geocryological data during the last several years have made it possible to achieve very close agreement between empirical (Heginbottom et al., 1993) and computed (Anisimov et al., 1995; Anisimov and Nelson, 1996, 1997) maps of modern permafrost.

Nelson and Anisimov (1993) and Anisimov and Nelson (1996, 1997) used the frost index in conjunction with several climatic scenarios to estimate changes in permafrost zonation caused by warming of the global climate in the first half of the next century. Climatic scenarios were based on paleoreconstructions and several general circulation models (GCMs). Although they differed in regional details, several transient GCMs predicted significant warming in the permafrost regions, and an attendant reduction of the area underlain by permafrost by an amount ranging between 12 and 22% (Anisimov and Nelson, 1997). The maps presented in these studies give insight into the magnitude of geocryological impacts of climate change in the first half of the next century. The method used for predictive mapping does not, however, take into account the lag between the reaction of the upper layer and deep permafrost, and the maps are best interpreted as representing *potential* permafrost distribution, realizable only after a protracted period under the new climatic regime.

Riseborough and Smith (1993) simulated the dynamics of permafrost thinning at a location in subarctic Canada and found that 5 m of marginal permafrost would thaw in less than 70 years under a climate-change scenario generated by the Canadian Climate Center GCM. In areas with thick, ice-rich permafrost (e.g., West Siberia), however, retreat of permafrost zones under the same climatic forcing would be much slower (Riseborough, 1990). Because the frost index does not involve a dynamic component, it can treat such effects only on a qualitative level.

The problem of thermal inertia in geocryological prediction does not arise when only near-surface processes are considered, on an annual basis. In permafrost environments the active layer is the only component of the substrate in which major changes can occur in its physical properties during each annual cycle. In areas underlain by unconsolidated sediments, these changes may involve variations of ice/water content, thermal conductivity, density, and mechanical properties. Such variations are of critical importance for many natural phenomena and processes (e.g., vegetation, water balance, cryogenic processes), and impose serious restrictions on land use, agriculture, and construction. Studies of the active layer therefore have large implications for ecology and cold-regions engineering.

Many factors affect active-layer thickness. Among the most important are air temperature, annual surface temperature amplitude, duration of the warm period, snow depth, vegetation, soil water/ice content, the thermal properties of soil, and the near-surface organic layer. Depending on local conditions, active-layer thickness may vary by a factor of two or even more over distances involving only tens of meters (Nelson et al., 1997a,b).

Interannual variations of active-layer thickness are strongly dependent on air temperature, a regional-scale variable subject to change over the next century.

Relations between the active layer and climatic factors are best known for the Russian permafrost regions, and maps for contemporary conditions are available for the Yamal Peninsula, West Siberia, Yakutia, and the Far East, where empirical studies have been conducted continuously over the last several decades (Pavlov, 1976; Shkadova, 1979; Ershov, 1989). In North America, active-layer observations have been less regular. Although these data are of great importance for understanding contemporary conditions in the permafrost regions, they are not sufficient for drawing conclusions about changes in the active layer under global warming. Because active-layer thickness is a response primarily to meteorological events associated with a single annual cycle, it can be treated using relatively simple models that do not account for complex interactions between changing atmospheric parameters and the thermal regime in deep permafrost. Instead, they are based on current climatic statistics and scenarios of climate change.

3. Active-layer modeling

Many attempts have been made to model climate–permafrost interactions, and to predict active-layer thickness theoretically. One of the most straightforward approaches is based on a simplified version of Stefan's solution for the heat-transfer problem in a solid medium (e.g., Jumikis, 1977; Mackay, 1995). Another extreme is represented by complex numerical models that account for many of the processes involved in the climate–permafrost system, and are capable of calculating gradual changes in active-layer thickness within given temporal intervals (e.g., Anisimov, 1989; Waelbroeck, 1993). None of these models is appropriate for the purposes of this study; Stefan's formulations are oversimplified and complex models require more input information than can be supplied in the context of the hemispheric scale addressed in this paper.

An alternative to these approaches is adaptation of a semi-empirical method developed in Russia primarily for the practical needs of cold-regions engineering, but adjusted to operate at the hemispheric scale. The fundamentals of the method were formulated over a longer period at Moscow State University (summarized by Kudryavtsev et al., 1974), developed further by Ershov (1971) and Garagulya (1990), and discussed by other investigators (e.g, Romanovsky and Osterkamp, 1995). Kudryavtsev's formulations are used in this study to model the active layer, taking into account the effects of snowcover, vegetation, soil moisture, and soil thermal properties. The model allows calculation of active-layer thickness and surface temperatures under a wide variety of climatic conditions.

Kudryavtsev's method assumes that annual variations of the air temperature can be described by the periodic function:

$$T_a(t) = \overline{T}_a + A_a \cos(2(t/P)) \tag{1}$$

where A_a is the annual amplitude of the air temperature, $\overline{T}_a$ is mean annual air temperature, t is time, and P is the period of the temperature cycle (1 yr). The layer of mineral soil is considered to be a homogeneous medium with different thermal properties in the frozen and thawed states; this layer underlies three additional layers: an organic-rich surface horizon, vegetation, and snow. The following semi-empirical equation for the depth of seasonal thawing or freezing can be applied (Kudryavtsev et al., 1974):

$$Z = \frac{2\left(A_s - \overline{T}_z\right)\cdot\left(\frac{\lambda\cdot P\cdot C}{\pi}\right)^{1/2} + \frac{\left(2A_z\cdot C\cdot Z_c + Q_L\cdot Z\right)\cdot Q_L\left(\frac{\lambda\cdot P}{\pi\cdot C}\right)^{1/2}}{2A_z\cdot C\cdot Z_c + Q_L\cdot Z + \left(2A_z\cdot C + Q_L\right)\cdot\left(\frac{\lambda\cdot P}{\pi\cdot C}\right)^{1/2}}}{2A_zC + Q_L} \tag{2}$$

where

$$A_z = \frac{A_s - \bar{T}_z}{\ln\left(\frac{A_s Q_L/2C}{\bar{T}_z + Q_L/2C}\right)} - \frac{Q_L}{2C} \tag{3}$$

and

$$Z_c = \frac{2(A_s - \bar{T}_z)\cdot\left(\frac{\lambda \cdot P \cdot C}{\pi}\right)^{1/2}}{2A_z \cdot C + Q_L} \tag{4}$$

Z is the depth of freezing or thawing (m); A_s is the annual amplitude of the surface temperature (°C); $\bar{T}_z$ is the mean annual temperature at the depth of seasonal thawing (°C); λ and C are the thermal conductivity and volumetric heat capacity of the soil (W m^{-1} $°C^{-1}$, and J m^{-3} $°C^{-1}$); P is the period of the annual temperature cycle (1 yr, expressed in seconds); and Q_L is the volumetric latent heat of fusion (J m^{-3}).

Eq. (2) includes mean annual soil temperature and soil temperature amplitude. Problems arise in parameterizing the transfer of energy to the surface and soil levels; owing to the complex effects of turbulence, radiative energy exchange, and variations in snow cover and vegetation, the mean annual air temperature in permafrost regions may be several degrees lower than the corresponding surface temperature. Kudryavtsev et al. (1974) suggested considering the thermal regime independently at several levels: (a) the boundary between the atmosphere and the seasonal surface cover (in the present study the annual surface temperature and amplitude are assumed equal to those in the air); (b) the soil surface under snow and vegetation; and (c) the temperature at the top of the permafrost.

Kudryavtsev's method evaluates the contribution of each component factor to the total air–soil temperature difference, expressing temperature and amplitude at the soil surface as:

$$\begin{aligned} \bar{T}_s &= \bar{T}_a + \Delta T_{sn} + \Delta T_{veg} \\ A_s &= A_a - \Delta A_{sn} - \Delta A_{veg} \end{aligned} \tag{5}$$

$\bar{T}_s$ and A_s are the mean annual temperature and amplitude at the soil surface, and ΔT_{sn}, ΔA_{sn}, ΔT_{veg}, and ΔA_{veg} are adjustments for the thermal effects of snow and vegetation.

Temperature at the depth of seasonal thawing can be expressed as:

$$T_z = T_s + \Delta T_\lambda \tag{6}$$

where ΔT_λ is the thermal offset resulting from the different thermal properties of the frozen and thawed soil.

The empirical equation accounting for the warming effect of snowcover has the form (Kudryavtsev et al., 1974):

$$\Delta T_{sn} = A_a\left\{1 - \exp\left[-Z_{sn}\left(\frac{\pi \cdot C_{sn}\,\rho_{sn}}{P \cdot \lambda_{sn}}\right)^{1/2}\right]\right\} \tag{7}$$

where Z_{sn} is snowcover thickness (m); λ_{sn} is the snow's thermal conductivity; C_{sn} is its specific heat capacity (J kg^{-1} $°C^{-1}$); and ρ_{sn} is snow density (kg m^{-3}).

To account for the thermal effects of vegetation the following equations are used (Ershov (1971):

$$\Delta A_{veg} = \frac{\Delta A_1 \tau_1 + \Delta A_2 \tau_2}{P} \tag{8}$$

$$\Delta T_{veg} = \frac{\Delta A_1 \tau_1 - \Delta A_2 \tau_2}{P} \cdot \frac{2}{\pi} \tag{9}$$

where τ_1 and τ_2 are the durations of the cold and warm periods, respectively (s); ΔA_1 and ΔA_2 are the differences between the average temperatures at the surfaces below and above the vegetation during the cold and warm periods (°C), expressed as

$$\Delta A_1 = \left(A_{veg} - \bar{T}_{veg}\right)\left\{1 - \exp\left[-Z_{veg}\left(\frac{\pi}{K^-_{veg} \cdot 2\tau_1}\right)^{1/2}\right]\right\} \tag{10}$$

$$\Delta A_2 = \left(A_{veg} + \bar{T}_{veg}\right)\left\{1 - \exp\left[-Z_{veg}\left(\frac{\pi}{K^+_{veg} \cdot 2\tau_1}\right)^{1/2}\right]\right\} \tag{11}$$

where

$$A_{veg} = A_a - \Delta A_{sn} \tag{12}$$

$$\bar{T}_{veg} = \bar{T}_a + \Delta T_{sn} \tag{13}$$

Z_{veg} is the height of the vegetation (m), and K^-_{veg} and K^+_{veg} represent its thermal diffusivity in the frozen and thawed states, respectively ($m^2\ s^{-1}$). This method allows estimation of the combined effect of snowcover and vegetation, and, depending on the snowcover thickness and duration of the cold period ΔT_{veg} can be either positive or negative, i.e., vegetation can have either cooling or warming effects on the ground thermal regime.

The mean annual temperature at the top of the permafrost was calculated using a semi-empirical equation (Garagulya, 1990):

$$\bar{T}_z = \frac{0.5 \cdot T_s \cdot (\lambda_f + \lambda_t) + A_s \dfrac{\lambda_t - \lambda_f}{\pi}\left[\dfrac{\bar{T}_s}{A_s}\arcsin\dfrac{\bar{T}_s}{A_s} + \left(1 - \dfrac{\pi^2}{A_s^2}\right)^{1/2}\right]}{\lambda *} \tag{14}$$

where

$$\lambda * = \begin{cases} \lambda_f, \text{ if numerator } < 0 \\ \lambda_t, \text{ if numerator } > 0 \end{cases}$$

and λ_t and λ_f are the thermal conductivities of thawed and frozen soil, respectively, ($W\ m^{-1}\ °C^{-1}$).

Volumetric heat capacity in the frozen (C_f) and thawed (C_t) states was calculated as:

$$\begin{aligned} C_f &= C \cdot \rho_s + 2025 \cdot w \\ C_t &= C \cdot \rho_s + 4190 \cdot w \end{aligned} \tag{15}$$

where C is the dry soil's heat capacity ($J\ kg^{-1}\ °C^{-1}$), ρ_s is the dry density of soil ($kg\ m^{-3}$), and w is relative soil moisture content, expressed as a decimal proportion.

The latent heat of phase change was calculated as:

$$Q_L = 335{,}200 \cdot w \tag{16}$$

Equations (1–16) allow calculation of the depth of seasonal freezing and thawing using data on air temperature, snowcover, vegetation, and soil thermal properties, and were used as a basis for mapping the thickness of the active layer under several scenarios of climatic change.

4. Validation

Although the ability of Kudryavtsev's formulation to predict the maximum depth of annual thawing and freezing has been tested extensively by different investigators (Kudryavtsev et al., 1974; Shkadova, 1979; Shur,

1988; Ershov, 1989), its application in this paper differs substantially from these studies, necessitating further validation. The main purpose of this exercise was to test its applicability to different time scales and environmental conditions. Data from several locations in the permafrost regions of the Northern Hemisphere with different climatic, vegetation and subsurface conditions were used to test the active-layer model.

Data from the Russian discontinuous permafrost zone incorporate observations from eleven meteorological stations with long records of soil temperature at different depths. Active-layer thickness was evaluated through the depth of the zero isotherm, obtained by interpolation of the soil temperature records at depths of 20, 40, 80, 160 and 320 cm and averaging over the observational period of 40 years (Pavlov, 1976; Shkadova, 1979).

To test the model's performance under more severe climatic conditions, three points in the Russian tundra (continuous permafrost) region with long records of thaw depth observations were employed. For these sites, the model was run with prescribed averages (over a 20 year period) of snow thickness, warm/cold season length, mean annual air temperature, and annual temperature amplitude. Representative soil types and values of soil moisture were used for each location (Ershov, 1989). Calculated values of the maximum depth of seasonal thawing were compared with active-layer data measured at the end of August, and averaged over eleven years.

Two locations in northern Alaska (Barrow and Happy Valley) with continuous annual records of air and soil temperature were used to analyze the ability of the model to predict the depth of seasonal thawing in particular years, and to describe interannual variations of active-layer thickness. Unlike the situation for the Russian sites, in which the model was driven by climatic normals, monthly air temperature and snow survey data for 1993 and 1994 were used for Barrow and Happy Valley. Soil parameters consistent with observations from these sites were employed in the calculation stream. Measured data consist of mean daily soil temperature records at depths of 0, 5, 10, 15, 20, 25, 30, 35, 45, 60, 90, and 120 cm (Nelson, unpublished data). This record was reinterpolated with a depth increment of 1 cm, and the maximum depth of the zero isotherm during the warm season was compared with output from the model.

Because actual vegetation data were not available for all locations, vegetation at each site used in the validation procedure was assumed to consist of a 10 cm layer of moss with thermal diffusivity equal to $1.39 \cdot 10^{-6}$ m^2 s^{-1} and $5.56 \cdot 10^{-8}$ m^2 s^{-1} in the frozen and thawed states, respectively (Kudryavtsev et al., 1974). Typical values of the soil thermal properties used for all calculations, obtained from Pavlov (1976), are shown in Table 1.

The calculated and measured maximum depths of thawing (or freezing for locations outside the permafrost regions) are compared in Fig. 2. Even under the very crude assumptions about soil thermal properties and vegetation used to run the active-layer model, the correspondence between calculated and measured values is very close. The relative deviation in most cases is below 10%, and does not exceed 20%. Nelson (1986) presented maps depicting the geographical consequences of varying soil thermal properties.

The model estimates active-layer thickness very accurately for Barrow in 1994 (39 cm modeled versus 37 cm predicted), but overestimates the value for 1993 (41 cm modeled, 29 cm measured). The mean annual air temperature in 1993 was 2°C higher than in 1994 (−10.8 in 1993 versus −12.9 in 1994); this difference is attributable entirely to higher winter temperatures. The minimum annual temperature in 1993 was 2.8°C higher

Table 1
Typical values for soil properties (Pavlov, 1976)

	Sand	Silt	Clay	Peat
Dry density (kg m^{-3})	1300	1400	1500	150
Heat capacity (J kg^{-1} $°C^{-1}$)	690	730	900	200
Thermal conductivity (W m^{-1} $°C^{-1}$)				
thawed (dry/wet)	1.05/2.15	1.05/1.90	0.90/1.70	0.35/0.60
frozen (dry/wet)	1.25/2.65	1.25/2.40	1.15/2.00	0.80/2.65

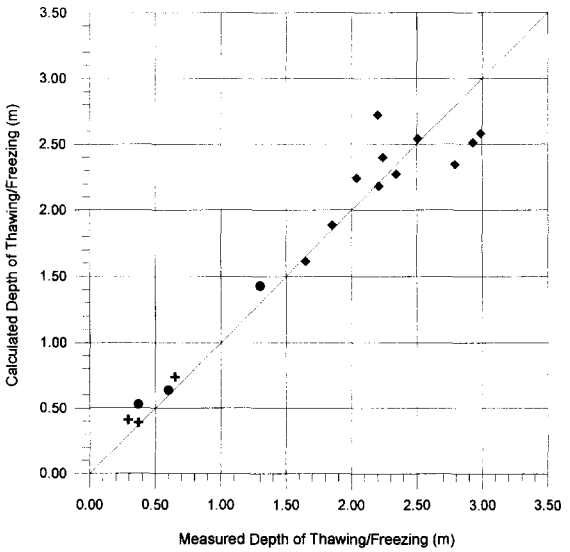

Fig. 2. Observed vs. calculated depths of seasonal thawing/freezing. Data were obtained from Shkadova, 1979 (diamonds); Ershov, 1989 (filled circles), and Nelson, unpublished (crosses).

than in 1994 (−25.7°C in 1993 and −28.5°C in 1994). The maximum annual temperatures were almost the same for both years (5.3°C in 1993, 5.6°C in 1994). The annual amplitude in 1993 was, therefore, 15°C, compared to 17°C in 1994; in combination with higher annual mean temperature, this factor led to overestimation of active-layer depth for 1993. This example illustrates that the model's accuracy may be lowered in some years with aberrant features in the annual air temperature cycle. Despite this shortcoming, which does not seriously affect the application detailed below, Kudryavtsev's solution provides effective estimates of the depth of seasonal thawing or freezing typical at particular locations, using climatic normals as input parameters.

5. Baseline climate and scenarios of climate change

Predictive mapping of active-layer thickness requires high-resolution climate data. The IIASA database (Leemans and Cramer, 1991) serves as an appropriate source of baseline data for comparison with climate-change scenarios from general circulation models. The IIASA database contains monthly normals of air temperature and precipitation from 13,118 weather stations in both hemispheres, interpolated onto a global grid with nodes spaced at 0.5° latitude/longitude intervals. The IIASA database was supplemented for this study with records from 800 additional Russian weather stations, providing a substantial improvement to the spatial coverage in the permafrost regions of West Siberia and the Far East. After reinterpolation, the expanded database was used as a baseline climate, against which all subsequent calculations were compared.

Predicted values for air temperature and precipitation under scenarios of future warming were calculated as sums of the baseline values and the expected increments estimated at each node from three transient coupled ocean–atmosphere GCMs. The climatic models used in this study are: (a) the GFDL89 model of the Geophysical Fluid Dynamic Laboratory (Manabe et al., 1991); (b) the ECHAM1-A model of the Max Plank Institute in Germany (Cubasch et al., 1992); and (c) the UKTR model of the United Kingdom Meteorological Office (Murphy, 1994; Murphy and Mitchell, 1994). Greco et al. (1994) provided extensive documentation for and intercomparisons of these models, as well as information about climate-change experiments for several temporal intervals, including the contemporary climate and the decade around 2050. The three models were

selected by Working Group II of the Intergovernmental Panel on Climate Change to provide a standard context for comparative impact studies.

Results from these experiments must be harmonized to account for the effects of 'climate drift', inconsistencies in the CO_2 emission scenarios used to drive each model, and different climate sensitivities. Climate drift is a computational effect arising when the model's control integrations produce values of the globally average air temperature that are different from those derived from weather records. To address this problem in the context of the present study, only relative changes of the climatic parameters predicted by GCMs have been considered, in conjunction with the empirical baseline data, to simulate future warmer climate.

To harmonize the models with respect to climate sensitivity and CO_2 emissions, the so-called 'simple linked' method was advocated by Greco et al. (1994). This adjustment involves preliminary calculations of the average global air temperature under a standardized CO_2 emissions scenario, using a simple one-dimensional climate model with given sensitivity to CO_2 doubling to further adjust the full-size GCM's results. More details about these procedures and comparison of the climatic scenarios are contained in Greco et al. (1994).

Anisimov and Nelson (1997) used the three GCMs, adjusted by the simple linked method, to study potential changes in permafrost distribution under climatic forcing. In the context of the problems addressed here, several conclusions are apparent:

(a) Although the ECHAM1-A and GFDL89 GCMs predict decreased seasonal or mean annual temperatures for the first half of the next century at some nodes in the mid-latitudes and subarctic, predictions for all high-latitude locations are positive and substantial (Greco et al., 1994).

(b) Temperature predictions from different GCMs and paleoreconstructions are in closer agreement for the high latitudes than for other regions (MacCracken et al., 1990; Shabalova and Seliakov, 1993; Anisimov and Nelson, 1996).

(c) The UKMO model predicts a more extreme warming for 2050 than do the other transient-mode GCMs employed in this study (Greco et al., 1994).

(d) The effects of climatic forcing by anthropogenic aerosols has not been considered adequately in these GCMs. Because they are regionally heterogeneous, sulphate aerosols may buffer the temperature increases predicted by many GCMs for high-latitude regions (Schneider, 1994; Blanchet, 1995; Mitchell et al., 1995; Santer et al., 1996; Schwartz and Andreae, 1996).

6. Scale / interpolation adjustments

The active-layer model was used with the IIASA climatic data set and the three scenarios of climate change to calculate the effects of warming on thaw depth by 2050. A major problem in this application is the lack of uniform coverage for many of the input data (snow, vegetation, soil thermal properties) at the hemispheric scale. Although the model yields good results for training sites at which it could be initialized accurately, uneven data coverage may produce patterns of active-layer thickness of variable quality over large regions. This problem was addressed through several adjustments:

6.1. Snow data

High-resolution data on snowcover thickness, density, and duration are not available at the hemispheric scale. Snowcover thickness was therefore calculated using air temperature and precipitation at each node. Spline interpolation of the monthly air temperature normals was used to calculate the beginning and end of the period with sustained freezing; any precipitation during this period is assumed to contribute to the snow depth (Nelson and Outcalt, 1987). An average winter snow depth $\bar{Z}_{sn}$ was calculated as

$$\bar{Z}_{sn} = \sin^2\phi \left\{ \sum_{i=1}^{k} \left[(P_i/\rho_r)(k-i+1) \right] / k \right\} \tag{17}$$

where k is the number of cold ($T_a \leq 0°C$) months, P_i is water-equivalent precipitation for the months i, and ρ_r is relative (dimensionless) snow density (assumed constant in this study at 0.3). The trigonometric term accounts for winter thaws, which are assumed to be shorter and less pronounced with increasing latitude ϕ. This parameterization was employed in several earlier studies, and yielded acceptable results in the permafrost regions (Nelson, 1986; Nelson and Anisimov, 1993; Anisimov and Nelson, 1996, 1997). The assumptions regarding geographic scale implicit in it were discussed by Nelson (1986, pp. 567–568). Stuart (1985) compared results from a variant of Eq. (17) with snow-depth observations from 199 Canadian stations, stratified by vegetation association. The equation accounted for 50–80% of the variance in the three data subsets.

6.2. Organic layer and vegetation data

Kudryavtsev's solution treats vegetation as an additional layer, with specific values of thermal conductivity in the cold and warm seasons. The parameterized formulas in the numerical algorithm were adjusted empirically using data from tundra regions. The best fit was achieved using a surficial layer of moss 10 cm thick. Unlike more complex permafrost models, the surface radiation balance and the turbulent heat flux, both of which are affected substantially by higher vegetation, were not considered in the model.

6.3. Subsurface data

Soil texture and moisture content vary substantially over short distances. This high-frequency variation, which is characteristic of soils in many regions (e.g., Webster and Oliver, 1990) makes it difficult to assign a single regionally representative value of soil thermal coefficients to each node. Because it is affected strongly by soil thermal properties and soil moisture, active-layer thickness is also highly variable over short distances (Nelson et al., 1997a,b). Computing series of maps for combinations of major soil categories and different moisture conditions provides an effective solution to this problem (e.g., Nelson, 1986, fig. 5; Research Institute for Engineering..., 1989) in the context of applied and impact studies.

7. Projected changes of active-layer thickness

Figs. 3 and 4 are hemispheric maps of contemporary active-layer depth calculated for sand, silt, and peat, and for different soil moisture conditions. Relative moisture content (ratio of the weights of water to dry soil) was ascribed to each soil type using typical observed values for years with low and high precipitation (Table 1). Thermal properties corresponding to particular values of soil moisture content (Table 1) were obtained from Pavlov (1976). Comparison of Figs. 3 and 4 demonstrates that the effect of changes in soil moisture on active-layer thickness is very substantial when silt soils are considered, less pronounced for sandy soils, and small in the case of soils with high organic content.

To minimize the effect of uncertainties in subsurface data on predicted active-layer thickness, differences between projected and current values were computed at each node using various combinations of subsurface parameter values (Table 1) and the transient GCMs for 2050 (Figs. 5 and 6). These maps show the relative increase in active-layer thickness (the difference between the projected and contemporary values divided by the contemporary, expressed in percent) for low (Fig. 5) and high (Fig. 6) soil moisture content. Values of soil moisture and thermal properties for each soil type are identical to those of Figs. 3 and 4. An arbitrary threshold of significance of 10% was imposed to eliminate possible computational effects lying within the accuracy of the method. Most of the expected changes in active-layer thickness shown in these figures are between 10% and 30%, falling into the first two categories of the maps. To achieve better visualization of the results, a nonuniform scale was used on the maps, with the third category (30–50% change) being twice the width of the preceding two.

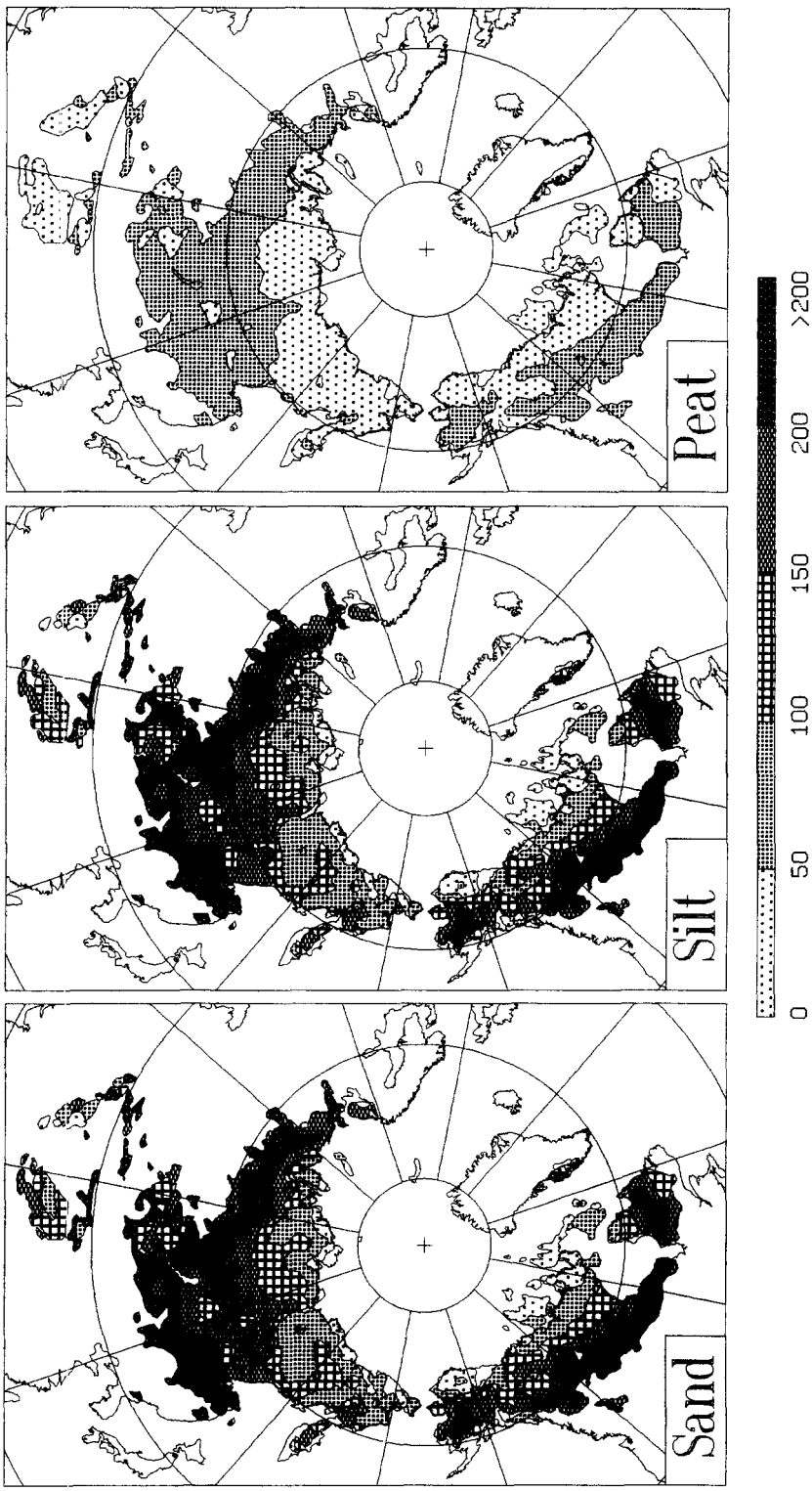

Fig. 3. Contemporary distribution of active-layer thickness (cm) in the Northern Hemisphere, computed using baseline climatic data from the IIASA database and typical soil properties for sand, silt and peat with low relative water content (0.15, 0.10, and 3.5 kg/kg).

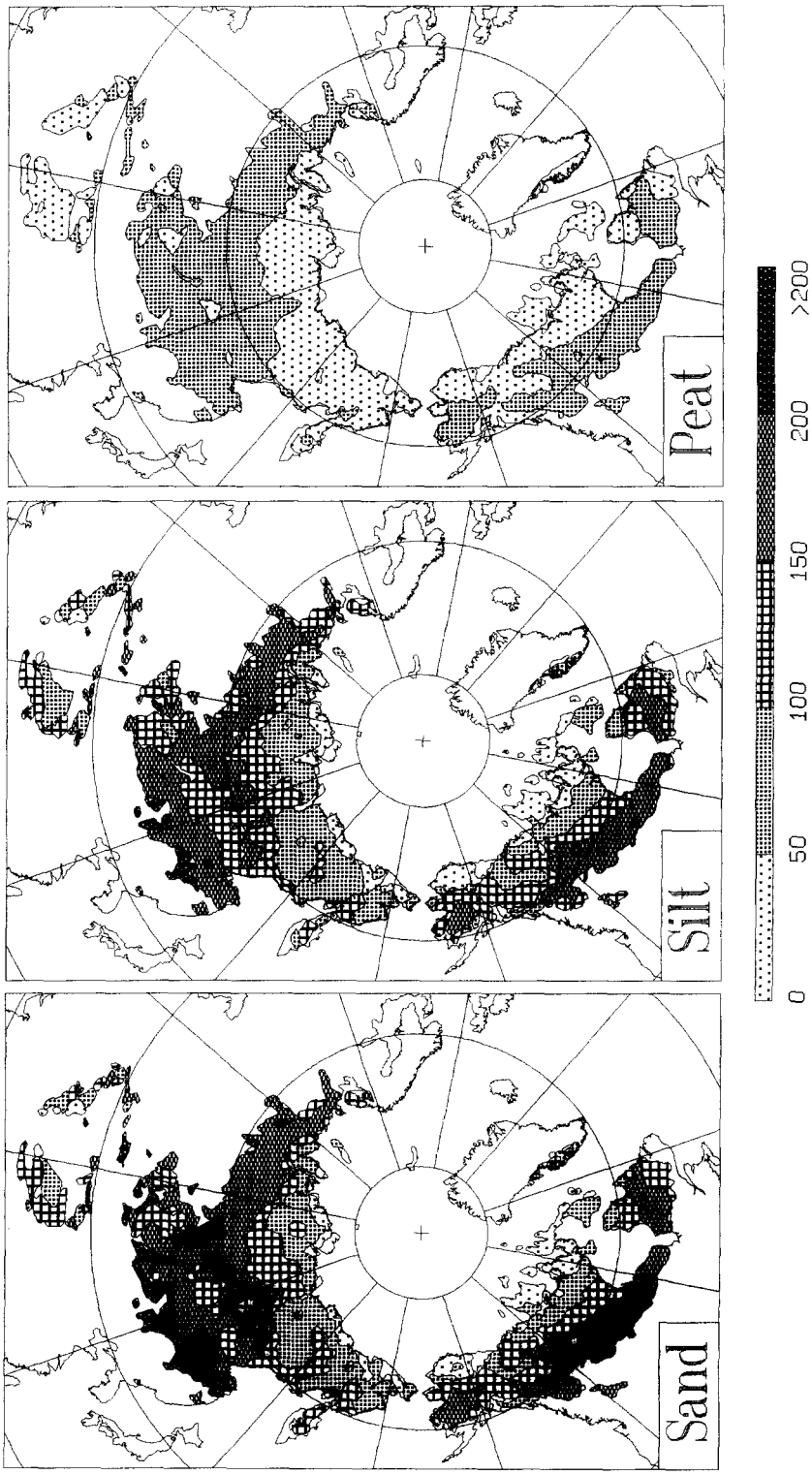

Fig. 4. Contemporary distribution of active-layer thickness in the Northern Hemisphere computed using IIASA baseline climatic data and typical soil properties for sand, silt and peat with high relative water content (0.35, 0.30, and 6.0 kg/kg).

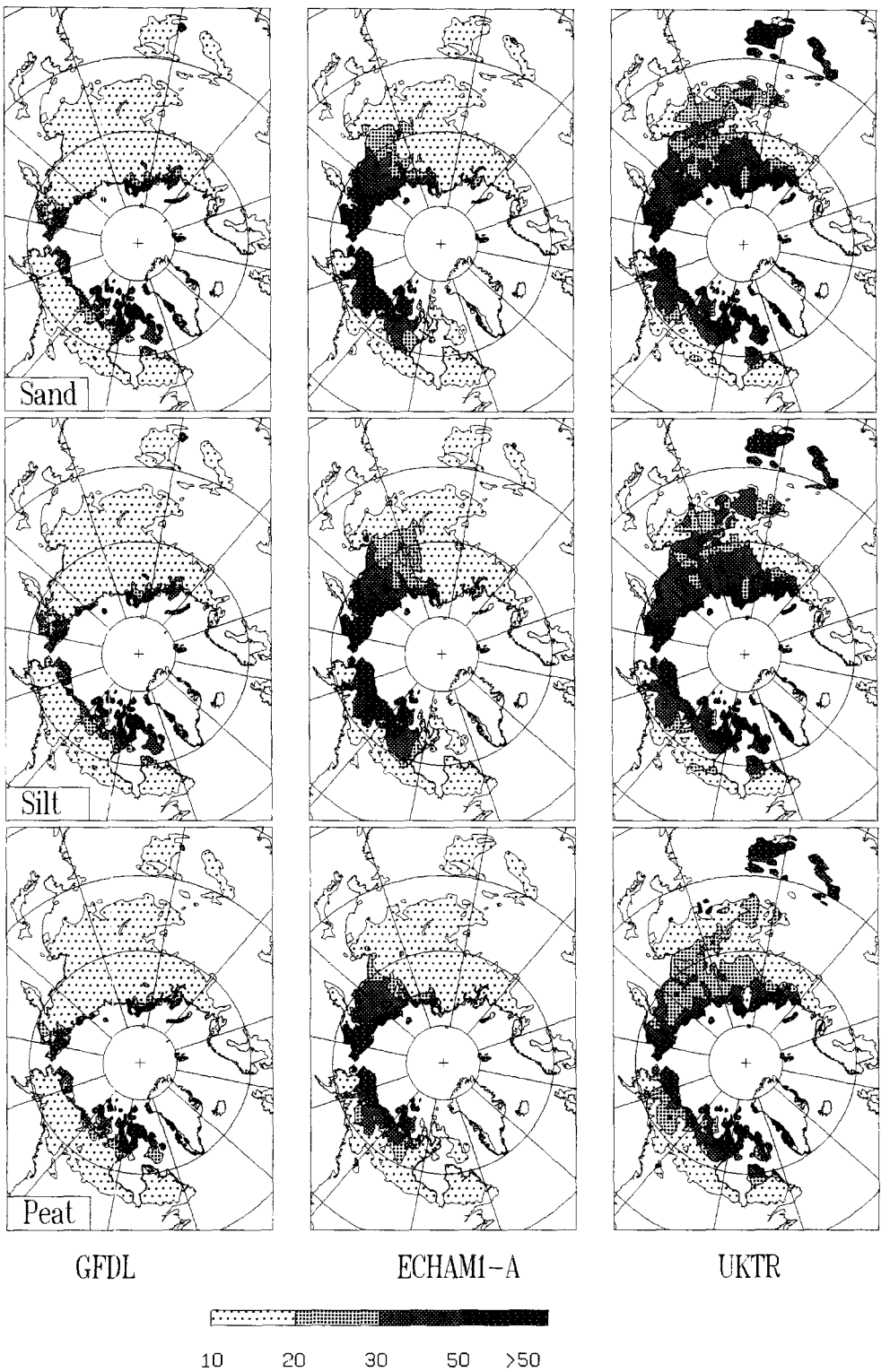

Fig. 5. Projected relative changes of active-layer thickness in the Northern Hemisphere computed using the GFDL89, ECHAM1-A, and UKTR scenarios of climate change for 2050 and typical soil properties for sand, silt and peat with low relative water content (0.15, 0.10, and 3.5 kg/kg).

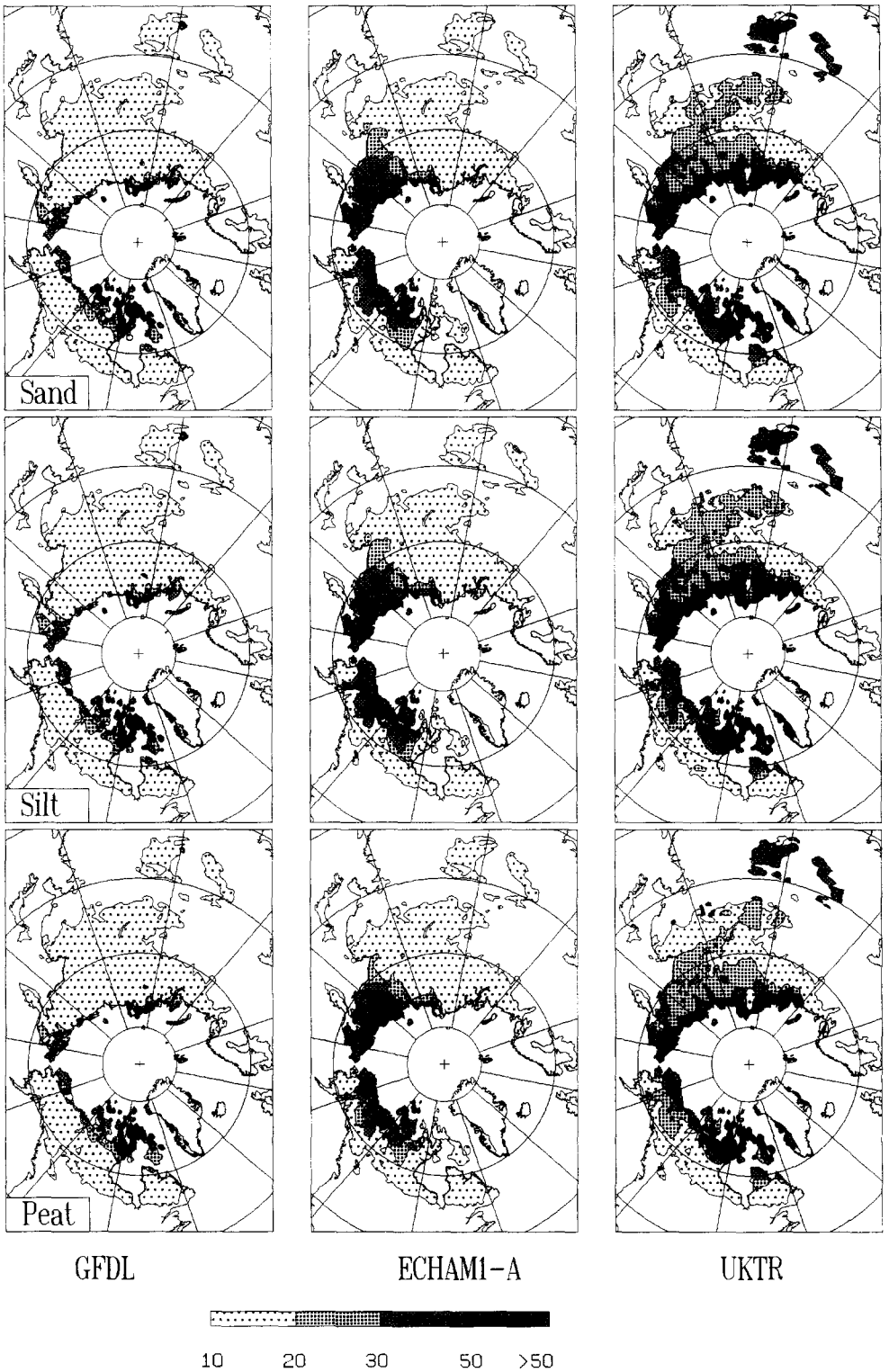

Fig. 6. Projected relative changes of active-layer thickness in the Northern Hemisphere computed using the GFDL89, ECHAM1-A, and UKTR scenarios and typical soil properties for sand, silt and peat with high relative water content (0.35, 0.30, and 6.0 kg/kg).

Although the three GCMs were scaled to the same degree of average global warming and reinterpolated to a common geographical lattice, they produce very different patterns of climatic change. Each of the scenarios also provides much richer regional detail than do those of the previous generation ($2 \times CO_2$) of general circulation models. Anisimov and Nelson's examination of potential changes in permafrost distribution under the GFDL89, ECHAM1-A, and UKTR GCMs scenarios (Anisimov and Nelson, 1997) included a discussion of regional changes produced by the different models. Some closely related patterns are apparent in Figs. 5 and 6.

The increase in active-layer thickness produced by the GFDL89 scenario is small compared to those yielded by the other GCMs. Pronounced changes (> 30%) are confined to the tundra regions, with the largest values concentrated in the Canadian Arctic Archipelago, the Russian Far East, and the Yamal/Gydan area of West Siberia. The pattern of changes produced by GFDL89 is rather similar for each of the soil-type/moisture-content categories.

In strong contrast with GFDL89, ECHAM1-A suggests that the largest relative increases in active-layer thickness will be concentrated in the Russian Far East and the western part of the North American Arctic. As with GFDL89, the pattern of changes produced by the GCM is similar for all combinations of soil type and moisture content.

The UKTR model predicts the most substantial warming in the Northern Hemisphere by 2050, and with respect to many impact studies it appears to be a rather extreme scenario. As is the case with permafrost distribution (Anisimov and Nelson, 1997), the UKTR scenario produces more pronounced changes in thaw depth than the other GCMs. Increases in relative values of active-layer thickness greater than 30% occur throughout the continuous and extensive discontinuous permafrost zones (cf. Anisimov and Nelson, 1997), as well as over most of the Tibet Plateau. The patterns of active-layer response produced by this scenario are dissimilar for mineral and for peat soils, with much more extensive changes occurring in central Asia, particularly for the drier of the prescribed conditions of soil moisture.

8. Conclusions

The changes represented in Figs. 5 and 6 would have serious impacts on the ecology, vegetation, engineering design, and construction practice in permafrost regions. The hemispheric scale adopted in this study has made it possible to provide some generalized insight into changes in active-layer thickness over the course of the first half of the next century. Many local details important for practical applications in engineering and ecology are, however, missing in the present research. Future work should take into consideration changes in vegetation associations that may result from warming (Myneni et al., 1997). Walker et al. (1997) have shown that in northern Alaska the depth of thaw is relatively shallow beneath moist acidic tundra, which may become more widespread under warmer conditions. This factor could offset atmospheric warming and lead to a general increase in the stability of permafrost within the affected area.

More detailed snow and subsurface data, including massive ground ice, will facilitate mapping the response of the active layer to anthropogenic warming at higher spatial resolutions. Incorporation of the effects of anthropogenic aerosols in the general circulation models may have a substantial buffering effect on active-layer thickness and will introduce additional regional complexity to maps at the scale presented here. Close investigation of the interplay in temporal scale between aerosol concentration and permafrost modification is, however, necessary for conclusive statements to be developed.

Acknowledgements

The research described in this publication was made possible in part by Award No. RG1-225 of the U.S. Civilian Research & Development Foundation for the Independent States of the Former Soviet Union (CRDF).

Support from the U.S. National Science Foundation is also gratefully acknowledged (Awards Nos. OPP-9612647 and OPP-9614537). We thank two anonymous reviewers for critical comments.

References

Andersland, O.B., Ladanyi, B., 1994. An Introduction to Frozen Ground Engineering. Chapman and Hall, New York, 352 pp.

Anisimov, O.A., 1989. Changing climate and permafrost distribution in the Soviet Arctic. Phys. Geogr. 10 (3), 285–293.

Anisimov, O.A., Nelson, F.E., 1996. Permafrost distribution in the Northern Hemisphere under scenarios of climatic change. Global Planet. Change 14 (1), 59–72.

Anisimov, O.A., Nelson, F.E., 1997. Permafrost zonation and climate change: results from transient general circulation models. Climatic Change 35, 241–258.

Anisimov, O.A., Nelson, F.E., Shiklomanov, N.I., 1995. Permafrost map of the Northern Hemisphere. Frozen Ground, 17 (cover illustration).

Blanchet, J.-P., 1995. Mechanisms of direct and indirect climate forcing by aerosols in the Arctic region. In: Charlson, R.J., Heintzenberg, J. (Eds.), Aerosol Forcing of Climate. Wiley, New York, pp. 109–121.

Budyko, M.I., Izrael, Y.A., 1987. Anthropogenic Climatic Change. Hydrometeoizdat, Leningrad, 405 pp. (in Russian; English edition published by Univ. Arizona Press, 1992).

Chapin, F.S. III, Jefferies, R.L., Reynolds, J.F., Shaver, G.R., Svoboda, J., 1992. Arctic Ecosystems in a Changing Climate: An Ecophysiological Perspective. Academic Press, San Diego, Calif., 469 pp.

Cubasch, U., Hasselmann, K., Hock, H., Maier-Reimer, E., Santer, B.D., Sausen, R., 1992. Time-dependent greenhouse warming computations with a coupled ocean–atmosphere model. Climate Dynamics 8, 55–69.

Ershov, E.D., 1971. Approximate quantitative estimate of the influence of various factors of the natural situation on the temperature regime of rocks. In: Merzlotnyye issledovaniya, 11. Izdatel'stvo MGU (Moscow State University; in Russian).

Ershov, E.D., 1989. Geocryology of the USSR. Nauka, Moscow (5 volumes; in Russian).

Fukuda, M., 1994. Methane flux from thawing Siberian permafrost (ice complexes)—results from field observations. Eos, Trans. Am. Geophys. Union 75 (44), 86.

Garagulya, L.S., 1990. Application of Mathematical Methods and Computers in Investigations of Geocryological Processes. Moscow Univ. Press, Moscow, 124 pp. (in Russian).

Greco, S., Moss, R.H., Viner, D., Jenne, R., Intergovernmental Panel on Climate Change, W.G. II, 1994. Climate Scenarios and Socioeconomic Projections for IPCC WG II Assessment. Consortium for International Earth Science Information Network, Washington, D.C., 12 pp. + maps, appendices, diskettes.

Heginbottom, J.A., Brown, J., Melnikov, E.S., Ferrians, O.J.J., 1993. Circumarctic map of permafrost and ground ice conditions. In: Proc. Sixth Int. Conf. Permafrost. South China Univ. Technol. Press, Wushan Guangzhou, pp. 1132–1136.

Jumikis, A.R., 1977. Thermal Geotechnics. Rutgers Univ. Press, New Brunswick, N.J., 375 pp.

Kudryavtsev, V.A., Garagulya, L.S., Kondrat'yeva, K.A., Melamed, V.G., 1974. Fundamentals of Frost Forecasting in Geological Engineering Investigations. Nauka, Moscow, 431 pp. (in Russian; English translation appears as U.S. Army Cold Regions Research and Engineering Laboratory Draft Translation 606).

Leemans, R., Cramer, W., 1991. The IIASA Database for Mean Monthly Values of Temperature, Precipitation, and Cloudiness on a Global Terrestrial Grid. Res. Rep. RR-91-18, Int. Inst. Applied Systems Analysis, Laxenburg, 62 pp.

MacCracken, M.C., Hecht, A.D., Budyko, M.I., Izreal, Y.A., 1990. Prospects for Future Climate: A Special US/USSR Report on Climate and Climate Change. Lewis Publishers, Chelsea, Mich., 270 pp.

Mackay, J.R., 1995. Active layer changes (1968 to 1993) following the forest–tundra fire near Inuvik, N.W.T., Canada. Arct. Alp. Res. 27 (4), 323–336.

Manabe, S., Stouffer, R.J., Spelman, M.J., Bryan, K., 1991. Transient responses of a coupled ocean–atmosphere model to gradual changes of atmospheric CO_2, Part I. Annual mean response. J. Climate 4 (8), 785–818.

Maxwell, J.B., Barrie, L.A., 1989. Atmospheric and climatic change in the Arctic and Antarctic. Ambio 1, 42–49.

Michaelson, G.J., Ping, C.-L., Kimble, J.M., 1996. Carbon storage and distribution in tundra soils of Arctic Alaska, U.S.A. Arct. Alp. Res. 28 (4), 414–424.

Mitchell, J.F.B., Davis, R.A., Ingram, W.J., Senior, C.A., 1995. On surface temperature, greenhouse gases, and aerosols: models and observations. J. Climate 8 (10), 2364–2386.

Murphy, J.M., 1994. Transient response of the Hadley Centre coupled ocean–atmosphere model to increasing carbon dioxide, Part I. Control climate and flux correction. J. Climate 8 (1), 36–56.

Murphy, J.M., Mitchell, J.F.B., 1994. Transient response of the Hadley Centre coupled model to increasing carbon dioxide, Part II. Spatial and temporal structure of response. J. Climate 8 (1), 57–80.

Myneni, R.B., Keeling, C.D., Tucker, C.J., Asrar, G., Nemani, R.R., 1997. Increased plant growth in the northern high latitudes from 1981 to 1991. Nature 386 (6626), 698–701.

Nelson, F.E., 1986. Permafrost distribution in central Canada: applications of a climate-based predictive model. Ann. Assoc. Am. Geogr. 76 (4), 550–569.

Nelson, F.E., Anisimov, O.A., 1993. Permafrost zonation in Russia under anthropogenic climatic change. Permafrost Periglacial Processes 4 (2), 137–148.

Nelson, F.E., Outcalt, S.I., 1987. A computational method for prediction and regionalization of permafrost. Arct. Alp. Res. 19 (3), 279–288.

Nelson, F.E., Lachenbruch, A.H., Woo, M.-K., Koster, E.A., Osterkamp, T.E., Gavrilova, M.K., Cheng, G.D., 1993. Permafrost and Changing Climate. In: Proc. Sixth Int. Conf. on Permafrost. South China Univ. Technol. Press, Wushan, Guangzhou, pp. 987–1005.

Nelson, F.E., Shiklomanov, N.I., Mueller, G., Hinkel, K.M., Walker, D.A., Bockheim, J.G., 1997a. Estimating active-layer thickness over a large region: Kuparuk River basin, Alaska. U.S.A. Arct. Alp. Res. 29(4), 367–378.

Nelson, F.E., Mueller, G.R., Shiklomanov, N.I., 1997b. Sampling designs for assessing variability of active-layer thickness. Abstr. 93rd Ann. Meet. Assoc. Am. Geogr., p. 191.

Pavlov, A.V., 1976. Thermophysics of Landscapes. Hydrometeoizdat, Leningrad, 276 pp. (in Russian).

Research Institute for Engineering Reconnaissance in Industrial Construction, 1989. Recommendations for the Forecast of Thermal Conditions in Frozen Ground. Stroizdat, Moscow, 72 pp. (in Russian).

Reynolds, J.F., Tenhunen, J.D., 1996. Landscape Function and Disturbance in Arctic Tundra. Springer, New York, 429 pp.

Riseborough, D.W., 1990. Soil latent heat as a filter of the climate signal in permafrost. In: Proc. Fifth Canadian Permafrost Conf. Centre d'etudes nordiques, Univ. Laval/National Research Council of Canada, Québec, pp. 199–205.

Riseborough, D.W., Smith, M.W., 1993. Modelling permafrost response to climate change and climate variability. In: Lunardinai, V.J., Bowen, S.L. (Eds.), Proc. Fourth Int. Symp. on Thermal Engineering and Science for Cold Regions. U.S. Army Cold Regions Research and Engineering Laboratory, Spec. Rep., 93-22, Hanover, NH, pp. 179–187.

Romanovsky, V.E., Osterkamp, T.E., 1995. Interannual variations of the thermal regime of the active layer and near-surface permafrost in northern Alaska. Permafrost Periglacial Processes 6 (4), 313–335.

Roots, E.F., 1989. Climate change: high latitude regions. Climatic Change 15 (1/2), 223–253.

Santer, B.D., Wigley, T.M.L., Barnett, T.P., Anyamba, E., 1996. Detection of climate change and attribution of causes. In: Houghton, J.T., Meira Filho, L.G., Callander, B.A., Harris, N., Kattenberg, A., Maskell, K. (Eds.), Climate Change 1995: The Science of Climate Change. Cambridge Univ. Press, Cambridge, pp. 407–443.

Schneider, S.H., 1994. Detecting climatic change signals: are there any 'fingerprints'?. Science 263 (5145), 341–347.

Schwartz, S.E., Andreae, M.O., 1996. Uncertainty in climate change caused by aerosols. Science 272 (5265), 1121–1122.

Shabalova, M.V., Seliakov, K.I., 1993. A model of regional climate changes based on paleoclimatic data. Meteorol. Gidrol. 7 (1): 35–43 (in Russian).

Shkadova, A.K., 1979. Soil Thermal Regime of the Territory of the USSR. Hydrometeoizdat, Leningrad, 240 pp. (in Russian).

Shur, Y.L., 1988. Upper Horizon of Permafrost and Thermokarst. Nauka, Moscow, 208 pp. (in Russian).

Stuart, A., 1985. The development of a spatial permafrost model for northern Canada and its application to scenarios of climate change. KelResearch Corporation, Downsview, Ont.

Waelbroeck, C., 1993. Climate–soil processes in the presence of permafrost: a systems modelling approach. Ecol. Modelling 69 (3,4), 185–225.

Walker, D.A., Auerbach, N.A., Bockheim, J.G., Chapin, F.S. III, Eugster, W., McFadden, J., Michaelson, G.J., Nelson, F.E., Ping, C.-L., Reeburgh, W.S., Regli, S., Shiklomanov, N.I., 1997. Moist nonacidic tundra: effects of substrate pH on land–atmosphere trace-gas and energy fluxes. In review.

Webster, R., Oliver, M.A., 1990. Statistical Methods in Soil and Land Resource Survey. Oxford Univ. Press, New York, 316 pp.

Weller, G., Chapin, F.S., Everett, K.R., Hobbie, J.E. eD, Kane, D., Oechel, W.C., Ping, C.L., Reeburgh, W.S., Walker, D., Walsh, J., 1995. The Arctic Flux Study: a regional view of trace gas release. J. Biogeogr. 22, 365–374.

Williams, P.J., 1995. Permafrost and climate change: geotechnical implications. Philos. Trans. R. Soc. London A 352 (1699), 347–358.